BRAIN CONNECTIVITY
Volume 11, Number 8, 2021

DOI: 10.1089/brain.2020.0866

Topological Aberrance of Structural Brain Network Provides Quantitative Substrates of Post-Traumatic Brain Injury Attention Deficits in Children

Meng Cao,[1] Yuyang Luo,[1] Ziyan Wu,[2] Catherine A. Mazzola,[3] Lori Catania,[4] Tara L. Alvarez,[1] Jeffrey M. Halperin,[5] Bharat Biswal,[1] and Xiaobo Li[1,2,i]

Abstract

Background: Traumatic brain injury (TBI)-induced attention deficits are among the most common long-term cognitive consequences in children. Most of the existing studies attempting to understand the neuropathological underpinnings of cognitive and behavioral impairments in TBI have utilized heterogeneous samples and resulted in inconsistent findings. The current research proposed to investigate topological properties of the structural brain network in children with TBI and their relationship with post-TBI attention problems in a more homogeneous subgroup of children who had severe post-TBI attention deficits (TBI-A).

Materials and Methods: A total of 31 children with TBI-A and 35 group-matched controls were involved in the study. Diffusion tensor imaging-based probabilistic tractography and graph theoretical techniques were used to construct the structural brain network in each subject. Network topological properties were calculated in both global level and regional (nodal) level. Between-group comparisons among the topological network measures and analyses for searching brain-behavioral were all corrected for multiple comparisons using Bonferroni method.

Results: Compared with controls, the TBI-A group showed significantly higher nodal local efficiency and nodal clustering coefficient in left inferior frontal gyrus and right transverse temporal gyrus, whereas significantly lower nodal clustering coefficient in left supramarginal gyrus and lower nodal local efficiency in left parahippocampal gyrus. The temporal lobe topological alterations were significantly associated with the post-TBI inattentive and hyperactive symptoms in the TBI-A group.

Conclusion: The results suggest that TBI-related structural re-modularity in the white matter subnetworks associated with temporal lobe may play a critical role in the onset of severe post-TBI attention deficits in children. These findings provide valuable input for understanding the neurobiological substrates of post-TBI attention deficits, and have the potential to serve as quantitatively measurable criteria guiding the development of more timely and tailored strategies for diagnoses and treatments to the affected individuals.

Keywords: attention deficits; diffusion tensor imaging; graph theory; pediatric; traumatic brain injury

Impact Statement

This study provides a new insight into the neurobiological substrates associated with post-traumatic brain injury attention deficits (TBI-A) in children, by evaluating topological alterations of the structural brain network. The results demonstrated that relative to group-matched controls, the children with TBI-A had significantly altered nodal local efficiency and nodal clustering coefficient in temporal lobe, which strongly linked to elevated inattentive and hyperactive symptoms in the TBI-A group. These findings suggested that white matter structural re-modularity in subnetworks associated with temporal lobe may serve as quantitatively measurable biomarkers for early prediction and diagnosis of post-TBI attention deficits in children.

Departments of [1]Biomedical Engineering and [2]Electrical and Computer Engineering, New Jersey Institute of Technology, Newark, New Jersey, USA.
[3]New Jersey Pediatric Neuroscience Institute, Morristown, New Jersey, USA.
[4]North Jersey Neurodevelopmental Center, North Haledon, New Jersey, USA.
[5]Department of Psychology, Queens College, City University of New York, New York, New York, USA.
The article was posted on June 12, 2020 by medRxiv, the preprint server for health sciences (https://doi.org/10.1101/2020.06.12.20129890).
[i]ORCID ID (https://orcid.org/0000-0002-8153-5415).

Introduction

Pediatric traumatic brain injury (TBI) is a major public health concern, which occurs in >100,000 children each year and incurs an estimated annual medical cost of >$1 billion (Watson et al., 2019). Neurocognitive impairments and behavioral abnormalities have been consistently observed in children with TBI (Dewan et al., 2016; Konigs et al., 2015; Lumba-Brown et al., 2018; Polinder et al., 2015). Among the most common cognitive consequences, significant attention deficits were reported in ~35% of children within 2 years of their TBI (Max et al., 2005), and were observed to strongly contribute to elevated risk for severe psychopathology and impairments in overall functioning in late adolescence, with the pathophysiological underpinning yet to be fully elucidated (Le Fur et al., 2019; Narad et al., 2019).

The post-TBI attention problems in children have been evaluated and treated based on endorsements of behavioral symptoms from subjective observations, and have resulted in largely divergent results regarding effectiveness (Backeljauw and Kurowski, 2014; Kurowski et al., 2019; LeBlond et al., 2019). Understanding the neurobiological substrates of post-TBI attention deficits (TBI-A) in children is thus vitally critical, so that timely and tailored strategies can be developed for diagnoses and long-term treatments and interventions.

In literature of pediatric TBI, injury-induced regional structural brain alterations and associated cognitive and behavioral impairments have been increasingly reported. Structural magnetic resonance imaging (MRI) studies have investigated the relationship between cortical thickness and functional outcomes in children with chronic TBI, and found that the abnormal cortical gray matter (GM) thickness in frontal, parietal, and temporal regions were significantly associated with working memory impairments (Merkley et al., 2008) and executive dysfunctions (Wilde et al., 2012b).

Existing diffusion tensor imaging (DTI) studies in children with TBI have also reported widespread white matter (WM) structural abnormalities and their linkage with post-TBI cognitive and behavioral impairments in the chronic stage. For instance, a number of DTI studies have demonstrated that disrupted WM integrity in corpus collosum (Ewing-Cobbs et al., 2008; Lindsey et al., 2019; Treble et al., 2013; Wilde et al., 2011), uncinate fasciculus (Lindsey et al., 2019), superior longitudinal fasciculus, and inferior fronto-occipital fasciculus (Dennis et al., 2015) were significantly associated with working memory impairments in children with TBI. Lower fractional anisotropy (FA) in frontal regions (Kurowski et al., 2009; Wozniak et al., 2007), superior longitudinal fasciculus and anterior corona radiata (Adamson et al., 2013), and ventral striatum (Faber et al., 2016) have been found to significantly link to post-TBI executive dysfunctions in children. Reduced FA in inferior longitudinal fasciculus, inferior fronto-occipital fasciculus, superior longitudinal fasciculus, and corpus callosum were also found to be associated with impaired attention function (Konigs et al., 2018).

The large inconsistency of these findings partially resulted from factors of the study samples, such as heterogeneity regarding TBI-induced cognitive and behavioral impairments and their severity levels, variations in terms of the biological and modifiable factors, differences in injury severity and mechanism, sample sizes, differences in imaging and data analysis techniques, and so on. In addition, for understanding relations of the anatomical and cognitive/behavioral alterations in TBI, the region-of-interest (ROI)-based investigations of the injured human brain can be biased without considering the fact that human brain is formed as a structurally and functionally connected network for information transferring.

Indeed, human brain regions do not work in an isolated manner. When processing sensory and higher-order cognitive information, cortical and subcortical brain regions have been found to dynamically reassemble into small-world networks, to maintain optimal communication efficiency (Bassett et al., 2011; Spreng et al., 2013). Structural connectome, facilitated by WM structural connectivity, has been highlighted to play important role in supporting functional brain processes (Baum et al., 2017; Chu et al., 2018).

A handful of studies involving adults with TBI have used graph theoretical techniques to explore the structural network alterations and have reported inconsistent results. Some studies reported significant structural network segregation in adults with TBI, including increased shortest path length and decreased global efficiency compared with controls (Caeyenberghs et al., 2014; Hellyer et al., 2015; Kim et al., 2014), whereas others reported no significant alterations in global network metrics (Caeyenberghs et al., 2013; Kuceyeski et al., 2019). One study found that the reduction of structural network connectivity at chronic stage might be related to the severity of injury, where adult with severe TBI demonstrated significant lower network topological measures than adult with mild TBI and controls (Raizman et al., 2020). A longitudinal study found that increased structural segregation was associated with better cognitive recovery within the patient group (Kuceyeski et al., 2019). The relationship between reduced structural network connectivity and cognitive impairment have also been observed in the group of professional fighters (Mishra et al., 2019). Relative to controls, adult TBI patients also demonstrated reduced structural connectivity in subnetworks that identified using network-based statistic (Dall'Acqua et al., 2017; Mitra et al., 2016).

In the context of pediatric TBI, structural brain network studies have found that children with TBI had altered global network properties. At acute and subacute stage, children with TBI were shown to have reduced global efficiency and increased clustering coefficient, characteristic path length, and modularity (Watson et al., 2019; Yuan et al., 2015, 2017b). For children with chronic TBI, the structural networks were found to have increased characteristic path length and decreased local efficiency, suggesting a more segregated, instead of a normally more coordinated, architecture for information processing, compared with matched controls (Caeyenberghs et al., 2012; Konigs et al., 2017; Yuan et al., 2017a). In addition, the reduced connectivity in the network was found to be associated with deficits in postural control (Caeyenberghs et al., 2012), and decreased intelligence quotient (IQ) and impaired working memory (Konigs et al., 2017) in TBI children. A longitudinal intervention study reported that improved overall cognitive performance after intervention was associated reduced network segregation in TBI children (Yuan et al., 2017a). A more recent study categorized the edges of the structural brain network into rich club (connections between different hubs), feeder (connections between hubs and other nodes),

and local (connections between different non-hub nodes) connections, and reported that children with TBI had significantly lower overall strength in rich club connections and higher overall strength in local connections; whereas none were associated with their significantly impaired executive function (Verhelst et al., 2018). Although increasing number of studies have started to focus their effort on understanding the relations of TBI-induced structural brain network alterations and cognitive/behavioral impairments (Imms et al., 2019), the neuroanatomical substrates of severe post-TBI attention deficits in children have not yet been fully investigated.

This study proposed to utilize the probabilistic tractography in DTI and graph theoretical techniques to assess the structural connectome properties in a carefully evaluated cohort of children with severe post-TBI attention deficits and group-matched controls. In previous functional MRI studies, significant functional hyperactivations in frontal and parietal regions have been consistently observed in children with TBI, during sustained attention and inhibitory control processes (Kramer et al., 2008; Strazzer et al., 2015; Tlustos et al., 2011). Based on these findings, we hypothesized that altered regional structural network properties in frontal and parietal areas may exist in children with severe post-TBI attention deficits.

Materials and Methods

Participants

A total of 66 children, including 31 with severe post-TBI attention deficits (TBI-A) and 35 group-matched controls, were initially involved in this study. A subject in the TBI-A group must have had a clinically diagnosed mild or moderate nonpenetrating TBI at least 6 months before the study date; and T score ≥65 in the inattention subscale (or T scores ≥65 in both inattention and hyperactivity subscales) in the Conners 3rd Edition-Parent Short form (Conners 3-PS) (Conners, 2008) assessed during the study visit. Children with TBI who had overt focal brain damages or hemorrhages were excluded. To rule out confounding factors associated with pre-TBI attention deficits, children who had a history of diagnosed attention-deficit/hyperactivity disorder (ADHD) (any subpresentations) before the diagnosis of TBI, or severe pre-TBI inattentive and/or hyperactive behaviors that were reported by a parent, were excluded from the TBI-A group. The control group included children with no history of diagnosed TBI, no history of diagnosed ADHD, and T scores ≤60 in all the subscales in the Conners 3-PS assessed during the study visit.

To further improve the homogeneity of the study sample, the general inclusion criteria for both groups included (1) only right-handed, to remove handedness-related potential effects on brain structures; (2) full scale IQ ≥80, to minimize neurobiological heterogeneities in the study sample; (3) ages of 11–15 years, to reduce neurodevelopment-introduced variations in brain structures. In the study, handedness was evaluated using the Edinburgh Handedness Inventory (Oldfield, 1971). Full scale IQ was estimated by the Wechsler Abbreviated Scale of Intelligence II (WASI-II) (Wechsler, 2011). The two groups were matched on sex (male/female) distribution and socioeconomic status (SES) that was estimated using the average education year of both parents.

The general exclusion criteria for both groups were (1) current or previous diagnosis of Autism Spectrum Disorders, Pervasive Development Disorder, psychotic, Major Mood Disorders (except dysthymia not under treatment), Post-Traumatic Stress Disorder, Obsessive-Compulsive Disorder, Conduct Disorder, Anxiety (except simple phobias), or substance use disorders, based on *Diagnostic and Statistical Manual of Mental Disorders*, *Fifth Edition* (DSM-5) (American Psychiatric Publishing, 2013) and supplemented by the Kiddie Schedule for Affective Disorders and Schizophrenia for School-Age Children—Present and Lifetime Version (K-SADS-PL) (Kaufman et al., 2000); (2) any types of diagnosed chronic medical illnesses, neurological disorders, or learning disabilities, from the medical history; (3) treatment with long-acting stimulants or nonstimulant psychotropic medications within the past month; (4) any contraindications for MRI scanning, such as claustrophobia, tooth braces, or other metal implants; (5) prepuberty subjects were also excluded, to reduce confounders associated with different pubertal stages (Blakemore and Choudhury, 2006). Puberty status was evaluated using the parent version of Carskadon and Acebo's self-administered rating scale (Carskadon and Acebo, 1993).

After initial processing of the neuroimaging data from each subject, three subjects were excluded from further analyses, owing to heavy head motion. Therefore, a total of 31 patients with TBI-A and 32 controls were included in group-level analyses.

The TBI-A subjects were recruited from the New Jersey Pediatric Neuroscience Institute (NJPNI), North Jersey Neurodevelopmental Center (NJNC), Children's Specialized Hospital (CSH), Brain Injury Alliance of New Jersey (BIANJ), and local communities in New Jersey. Controls were solicited from the local communities by advertisement in public places. The study received institutional review board approval at the New Jersey Institute of Technology (NJIT), Rutgers University, and Saint Peter's University Hospital. Before the study, all the participants and their parents or guardians provided written informed assents and consents, respectively.

Clinical/neurocognitive assessments and measures

Severity of TBI was characterized using the Glasgow Coma Scale (GCS) (Teasdale and Jennett, 1974), with the scores ranging from 9 to 15 in the TBI-A subjects. Severities of the inattentive and hyperactive/impulsive symptoms were dimensionally measured using the raw scores and T scores of the subscales in Conners 3-PS. The CogState brief battery for children (Eckner et al., 2011), which included five computerized tests, was administered to each subject. The normalized overall scores of the tests were used to evaluate neurocognitive capacities in executive function, psychomotor speed, visual attention, visual learning/memory and working memory.

All the demographic, clinical, and neurocognitive performance measures are given in Table 1.

Neuroimaging data acquisition protocol

MRI scans for each subject were performed on a 3-Tesla Siemens TRIO (Siemens Medical Systems, Germany) scanner at Rutgers University Brain Imaging Center. The DTI data were acquired using a single-shot echo planar sequence (voxel size = 2.0 mm × 2.0 mm × 2.5 mm voxel size, repetition

Table 1. Demographic, Clinical, and Neurocognitive Characteristics in the Study Sample

	Controls, mean (SD)	*TBI-A, mean (SD)*	*t or χ^2 value*	*p*
N	35 (M:18, F:17)	31 (M:16, F:15)	0.0002 (χ^2)	0.988
Age	13.83 (1.29)	14.13 (1.69)	−0.817	0.417
Ethnicity/race			0.2418 (χ^2)	0.886
Caucasian	25	23		
Hispanic	6	4		
Others	4	4		
Socioeconomic status	32.00 (3.70)	31.16 (4.16)	0.872	0.387
Full scale IQ	115.08 (11.27)	111.13 (12.59)	1.348	0.183
Conners 3rd Edition-Parent Short Form (T-score)				
Inattention	45.97 (5.86)	70.52 (7.32)	−18.031	<0.001
Hyperactivity/impulsivity	48.31 (5.55)	62.00 (14.08)	−6.546	<0.001
CogState Brief Neurocognitive Testing Battery				
Groton Maze Learning Test	106.34 (4.76)	105.58 (4.71)	0.653	0.516
Detection	100.54 (6.02)	101.39 (4.96)	−0.617	0.540
Identification	102.17 (5.25)	100.39 (6.68)	1.213	0.230
One Card Learning	101.34 (7.36)	100.16 (7.53)	0.644	0.522
One Back (Speed)	92.63 (9.18)	93.58 (10.61)	−0.391	0.697
One Back (Accuracy)	101.77 (6.94)	104.55 (8.20)	−1.490	0.141

F, females; IQ, intelligence quotient; M, males; *N*, no. of subjects; SD, standard deviation; TBI, traumatic brain injury; TBI-A, TBI attention deficit.

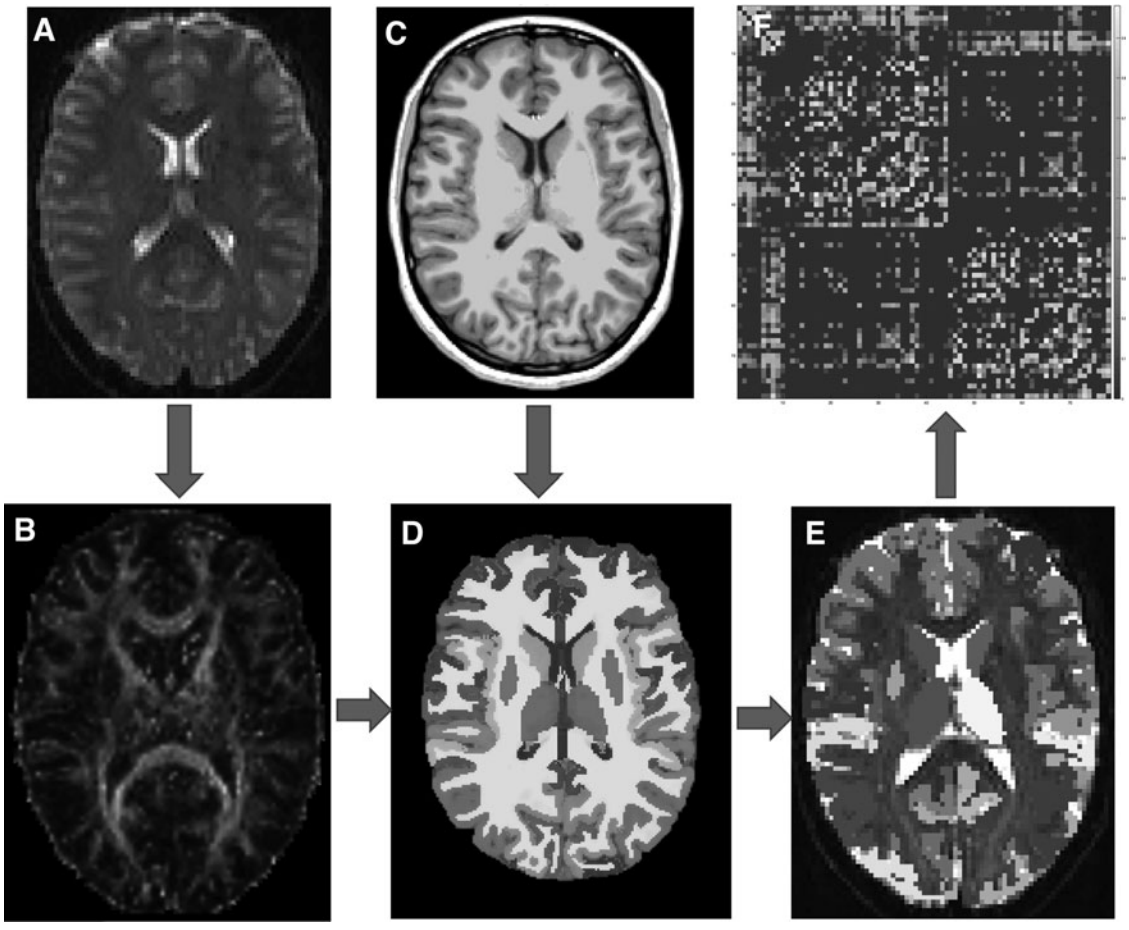

FIG. 1. Individual level imaging data analysis and network construction. **(A)** DTI data; **(B)** Estimated tensor directions with two-crossing fiber model; **(C)** T1-weighted structural MRI data; **(D)** Parcellated structural image based on Desikan–Killiany Atlas; **(E)** Seed masks in diffusion space, binarized, and transformed from structural space; **(F)** Symmetric and weighted 78×78 connectivity matrix. The edges were calculated based on the number of fibers in tractography. DTI, diffusion tensor imaging; MRI, magnetic resonance imaging.

time (TR) = 7700 msec, echo time (TE) = 103 msec, field of view (FOV) = 250 mm × 250 mm, 30 diffusion-sensitizing gradient directions with *b*-value = 700 sec/mm^2, and one image with *b*-value = 0 sec/mm^2). In addition, high-resolution T1-weighted data from each subject was also involved in the study for creation of individualized brain atlas. The T1-weighted anatomical images were obtained with a sagittal multi-echo magnetization-prepared rapid acquisition gradient echo sequence (voxel size = 1 mm^3 isotropic, TR = 1900 msec, TE = 2.52 msec, flip angle = 9°, FOV = 250 mm × 250 mm, and 176 sagittal slices).

Individual-level neuroimaging data preprocesses

DTI data preprocessing was performed using the Diffusion Toolbox from FMRIB Software Library v6.0 (FSL) (Jenkinson et al., 2012). Each DTI data (Fig. 1A as an example) was first manually checked for any missing slides or heavy geometric distortions. The head motions and eddy-current distortion were then corrected with affine transformation and predictions estimated by a Gaussian Process (Andersson and Sotiropoulos, 2016). Heavy head movement is a critical issue that can significantly affect the quality of imaging data and cause inaccurate results of tractography. In this study, the cutoffs of heavy head movements were defined as data with ≥2 mm translational displacement or ≥3° rotational displacement, with which data from three subjects were excluded from further analyses. Subjects involved in further analyses did not show significant between-group differences in the head movement measures (in mean translation [$t = 0.623$, $p = 0.536$], maximum translation [$t = 0.638$, $p = 0.526$], mean rotation [$t = 0.941$, $p = 0.350$], and maximum rotation [$t = 0.847$, $p = 0.400$]).

Nonbrain voxels were removed by performing brain extraction over the nondiffusion-weighted image (b0 image). The parameters for probabilistic tractography were estimated using the FSL/BedpostX toolbox (Behrens et al., 2007). This process estimated a two-fiber model in each voxel based on the probability distribution generated by Markov Chain Monte Carlo sampling (Fig. 1B).

In each subject, a total of 78 cortical and subcortical ROIs were generated from the T1-weighted data (Fig. 1C) using the standardized brain atlas parcellation procedures from FreeSurfer v6.0.0 (Fischl, 2012). There ROIs (Fig. 1D) included 68 cortical regions bilaterally, and 10 subcortical regions (bilateral putamen, caudate, hippocampus, thalamus, and pallidum). All the ROIs in structural space were linearly registered into each individual's native diffusion space by referencing to the b0 image and binarized into ROI masks to serve as seed masks for tractography (Fig. 1E).

Finally, the DTI probabilistic fiber tracking was performed using a streamline tractography algorithm, FSL/PROBTRACKX2. To prevent the generated fibers from running into GM and cerebrospinal fluid, a WM mask was used for the probabilistic tractography. Five thousand streamlines per voxel were then initiated from each seed mask, with 0.5 step distance. A fiber was terminated when (1) it reached other seed masks; (2) it exceeded 2000 step limits; (3) it looped back to the same streamline; (4) its curvature exceeded 80°; and (5) it left the WM mask. Once all fibers were terminated, fibers that reached one of the seed masks were retained and counted to determine the connectivity between ROIs.

Individual-level structural brain network construction and analyses

To construct the structural brain network for each subject, the 78 cortical and subcortical ROIs were used as network nodes. A pair of nodes was considered to have no anatomical connectivity (i.e., no edge in the network), if fiber tracts from neither of the two nodes successfully reached the other one, during the probabilistic tractography step. The weight of a nonzero edge was first evaluated by averaging the number of fibers on both directions. This raw value was then transformed using logarithm function and normalized by dividing the maximum edge weight in the same network (Rubinov and Sporns, 2011). In addition, a nonzero edge was further set as zero if at least 60% of the whole study sample had a zero weight on this edge (de Reus and van den Heuvel, 2013). This cutoff threshold was validated in previous studies for efficacy of controlling false-positive and false-negative rates of the generated connections (Bathelt et al., 2019; Misic et al., 2018; Verhelst et al., 2018). Then for each subject, the 78 × 78 symmetric connectivity matrix was generated for construction of the weighted structural brain (Fig. 1F).

The global and regional topological properties of the structural brain network from each subject were then estimated, including the network global and local efficiencies, network overall strength, and nodal global efficiency, nodal local efficiency, and nodal clustering coefficient of each node. All network topological property was calculated using Brain Connectivity Toolbox (Rubinov and Sporns, 2010).

The network global efficiency is a metric of the structural network integration that reflects the ability of information transferring across distributed brain areas (Latora and Marchiori, 2001). It was defined as

$$E_{glob}(G) = \frac{1}{n(n-1)} \sum_{i,j \in N, j \neq i} \frac{1}{d_{ij}}, \quad (1)$$

where d_{ij} was the inverse of the shortest distance between node i and j that was represented using the edge's normalized weight. When two nodes were not directly connected, the shortest distance was the sum of the shortest connecting edges.

The network local efficiency estimates the network segregation and represents the fault tolerance level of the network (Latora and Marchiori, 2001), which was defined as

$$E_{network-loc}(G) = \frac{1}{n} \sum_{i \in N} E_{glob}(G_i),$$

where G_i was the subnetwork consisted of all neighbor nodes of node i, and the global efficiency of subnetwork G_i is calculated using Equation (1).

The network overall strength was defined as the average of the normalized weights of the edges in the network, which was used to represent the overall connectivity of the network.

The nodal global efficiency of node i is a measure of its nodal communication capacity with all other nodes in the network, which was defined as

$$E_{nodal}(i) = \frac{1}{n-1} \sum_{j \in N, j \neq i} \frac{1}{d_{ij}}.$$

Nodal local efficiency of node i represents the robustness and integration of the subnetwork it belongs, which was defined as the global efficiency of the subnetwork consist of all the neighbors of i.

The nodal clustering coefficient describing the likelihood of whether the neighboring nodes of node i are interconnected with each other (Onnela et al., 2005). It was defined as

$$C(i) = \frac{1}{k_i(k_i-1)} \sum_{j,h \in N_i} \left(w_{ij} w_{ih} w_{jh}\right)^{1/3},$$

where j, k were neighbors of node i, and k_i was the number of neighbors of node i.

In a communicative network, there are certain nodes that have strong connections with other nodes, and/or frequently appear in the shortest between-node paths. These critical nodes are called ''network hubs,'' which serve to connect multiple segregated subnetworks and facilitate the intermodular integrations (Rubinov and Sporns, 2010). In our study, nodal strength and betweenness centrality (BC) were estimated to characterize the hub property of each node in a network. The strength of a node was defined as the sum of the weights of its edges; whereas the BC attempted to measure the ability for one node to bridge indirectly connected nodes (Freeman, 1978). BC was defined as

$$BC(i) = \frac{1}{(n-1)((n-2)} \sum_{j,k \in N,\ j \neq k} \frac{p(i \mid j,k)}{P(j,k)},$$

where j, k were node pairs in the network. $p(i|j,k)$ was whether the shortest path between node j and node k passes through node i. $P(i,k)$ was the total number of unique shortest path between node j and node k.

For each node in a WM structural brain network, its nodal global efficiency represents the integration of its associated WM structural subnetworks; whereas its nodal local efficiency and nodal clustering coefficient represent the modularity, and BC represents the connectivity of its associated WM subnetworks (Fagerholm et al., 2015; Jolly et al., 2020).

Group-level analyses

Group statistics were carried out using SPSS 25 on macOS Mojave 10.14.1. Between-group comparisons in demographic, clinical, behavioral, and neurocognitive performance measures were conducted using chi-square test for categorical data (sex and ethics), and independent two sample t-test for numerical measures.

Group comparisons in the network topological measures were performed using a mixed-effects general linear model by setting TBI-A and controls as group variables, and adding IQ, age, SES as random-effect, and sex as fixed-effect covariates, respectively. In addition, the group-specific network hubs of each diagnostic group were examined using one-sample t-test in the nodal strength and BC measures, respectively, with a threshold of 2 standard deviations higher than the group mean. Group comparisons in all these network measures were controlled for potential multiple comparisons (in the total of 78 network nodes), using Bonferroni correction with a threshold of significance at corrected $\alpha \leq 0.05$ (Green and Diggle, 2007).

Brain-behavior relationships in the TBI-A group were assessed using Pearson correlation between the T scores of the inattentive and hyperactive/impulsive subscales from Conners 3-PS and the network measures that showed significant between-group differences. The correlation analyses were controlled for potential multiple comparisons (in the total number of comparisons), by using Bonferroni correction with a threshold of significance at corrected $\alpha \leq 0.05$.

Results

Demographic, clinical/behavioral, and neurocognitive performance measures

As given in Table 1, there were no significant between-group differences in the demographic and neurocognitive performance measures. Compared with the controls, the children with TBI-A showed significantly more inattentive ($p < 0.001$) and hyperactive/impulsive ($p < 0.001$) symptoms measured using the T scores in Conners 3-PS.

Topological properties of the structural brain network

The global network properties did not show significant between-group differences. Compared with controls, the TBI-A group showed significantly increased nodal local efficiency ($p = 0.005$) and nodal clustering coefficient ($p < 0.001$) in left inferior frontal gyrus; significantly increased BC ($p = 0.037$) in left superior frontal gyrus; and significantly increased nodal local efficiency ($p = 0.036$) and nodal clustering coefficient ($p = 0.043$) in right transverse temporal gyrus. Meanwhile, relative to controls, the TBI-A group also demonstrated significantly decreased nodal local efficiency ($p = 0.026$) in left parahippocampal gyrus; and greatly reduced nodal clustering coefficient ($p = 0.017$) in left supramarginal gyrus (Table 2).

Table 2. Anatomical Regions That Showed Significant Between-Group Differences in Nodal Topological Properties of the Structural Brain Network

Anatomical region	*Measurement*	*Controls, mean (SD)*	*TBI-A, mean (SD)*	*F*	*p-After Bonferroni correction*
Left inferior frontal gyrus	Nodal local efficiency	0.397 (0.041)	0.437 (0.042)	16.738	0.005
	Nodal clustering coefficient	0.326 (0.048)	0.376 (0.043)	20.879	<0.001
Right transverse temporal gyrus	Nodal local efficiency	0.420 (0.064)	0.478 (0.062)	12.128	0.036
	Nodal clustering coefficient	0.412 (0.063)	0.471 (0.061)	11.736	0.043
Left parahippocampal gyrus	Nodal local efficiency	0.534 (0.058)	0.489 (0.042)	12.834	0.026
Left supramarginal gyrus	Nodal clustering coefficient	0.519 (0.050)	0.476 (0.045)	13.802	0.017
Left superior frontal gyrus	Betweenness centrality	0.100 (0.032)	0.127 (0.030)	12.044	0.037

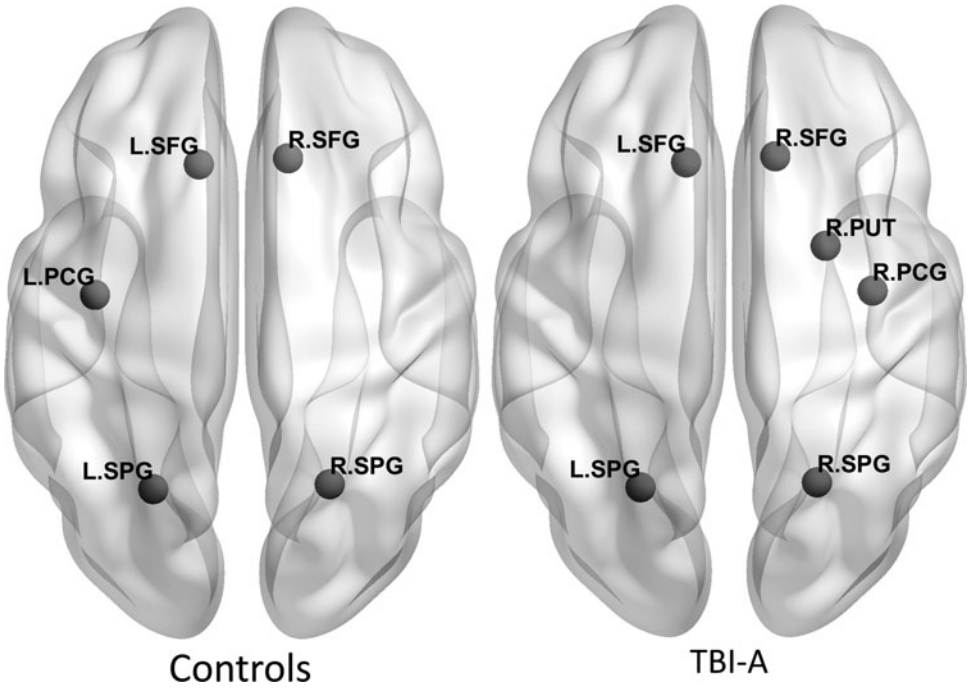

FIG. 2. Network hubs identified using the BC measure in the groups of controls and TBI-A. PCG, precentral gyrus; PUT, putamen; L, left hemisphere; R, right hemisphere; SFG, superior frontal gyrus; SPG, superior parietal gyrus; TBI-A, TBI-attention deficits.

In addition, distinct patterns of the within-group hub distribution were observed in the two diagnostic groups (Fig. 2), with the precentral gyrus and putamen nucleus in the right hemisphere showing as hubs (measured by BC) in the TBI-A group but not in controls. Left precentral gyrus was identified as a hub in controls but not in the TBI-A group.

Brain-behavior relationships in the TBI-A group

In the TBI-A group, increased nodal local efficiency of left parahippocampal gyrus was significantly associated with increased inattentive ($r=0.405$, $p=0.024$) and hyperactive/impulsive ($r=0.457$, $p=0.01$) symptoms, whereas greater nodal clustering coefficient of right transverse temporal gyrus was strongly associated with decreased hyperactive/impulsive symptoms ($r=-0.468$, $p=0.008$) (Fig. 3).

Discussion

This study depicted for the first time that aberrant regional topological properties of the WM structural brain network play critical role in severe post-TBI-A in children. Specifically, we found that relative to the group-matched controls, children with TBI-A had significantly increased nodal local efficiency and nodal clustering coefficient in the left inferior frontal gyrus, as well as significantly higher BC in the left superior frontal gyrus. These results suggest significantly increased structural connectivity and modularity of the subnetworks associated with left inferior and superior frontal gyri in children with severe post-TBI attention deficits. Chronic tissue abnormalities in children with mild and moderate TBI have been found to be mainly resulted from diffuse axonal injury (DAI), owing to the abrupt stretching, twisting, and shearing of axons in the event of a mechanical blow (Roberts et al., 2016). Frontal lobe, located class to the anterior fossa of the skull, is one of the most vulnerable brain regions to DAI (Bigler, 2007). Existing neuroimaging studies in children with chronic TBI have consistently demonstrated structural anomalies in frontal cortex GM and the WM pathways connect it and other brain regions. For instance, multiple structural MRI and DTI studies have reported frontal GM volumetric reduction and cortical thinning (Bigler et al., 2013; Dennis et al., 2016; Mayer et al., 2015; Wilde et al., 2012b), as well as disrupted frontal WM integrity, represented by reduced WM FA and increased apparent diffusion coefficient in children with chronic TBI relative to group-matched controls (Wilde et al., 2011, 2012a; Wozniak et al., 2007). Frontal tissue anomalies in children with TBI have also been found to link to long-term neurobehavioral impairments in domains such as executive control (Lipszyc et al., 2014) and learning and memory (Lindsey et al., 2019), whereas no evidence from previous quantitative clinical and neuroimaging studies have suggested strong correlations between frontal GM/WM tissue alterations and post-TBI attention deficits in children. Along with these existing studies, results from this study suggest that abnormal structural connectivity and modularity of the subnetworks associated with frontal lobe may be caused by TBI-induced structural damages in frontal cortex and associated WM structures, whereas these regional topological alterations of the WM structural network might not necessarily play the key role in long-term and severe post-TBI attention deficits in the affected individuals.

Compared with controls, the TBI-A group demonstrated significantly reduced nodal clustering coefficient in left supramarginal gyrus. This result of reduced topological modularity of the structural subnetwork in parietal regions is consistent with findings from a previous structural network study using deterministic tractography (Caeyenberghs et al., 2012). In addition, several previous DTI studies in children with chronic TBI have consistently reported significantly decreased FA of the superior longitudinal fasciculus, which is a major association tract that connects parietal lobe with frontal lobe (Ewing-Cobbs et al., 2016; Konigs et al., 2018; Molteni et al., 2019). An early structural MRI study reported significantly reduced cortical thickness of bilateral supramarginal gyri in children with

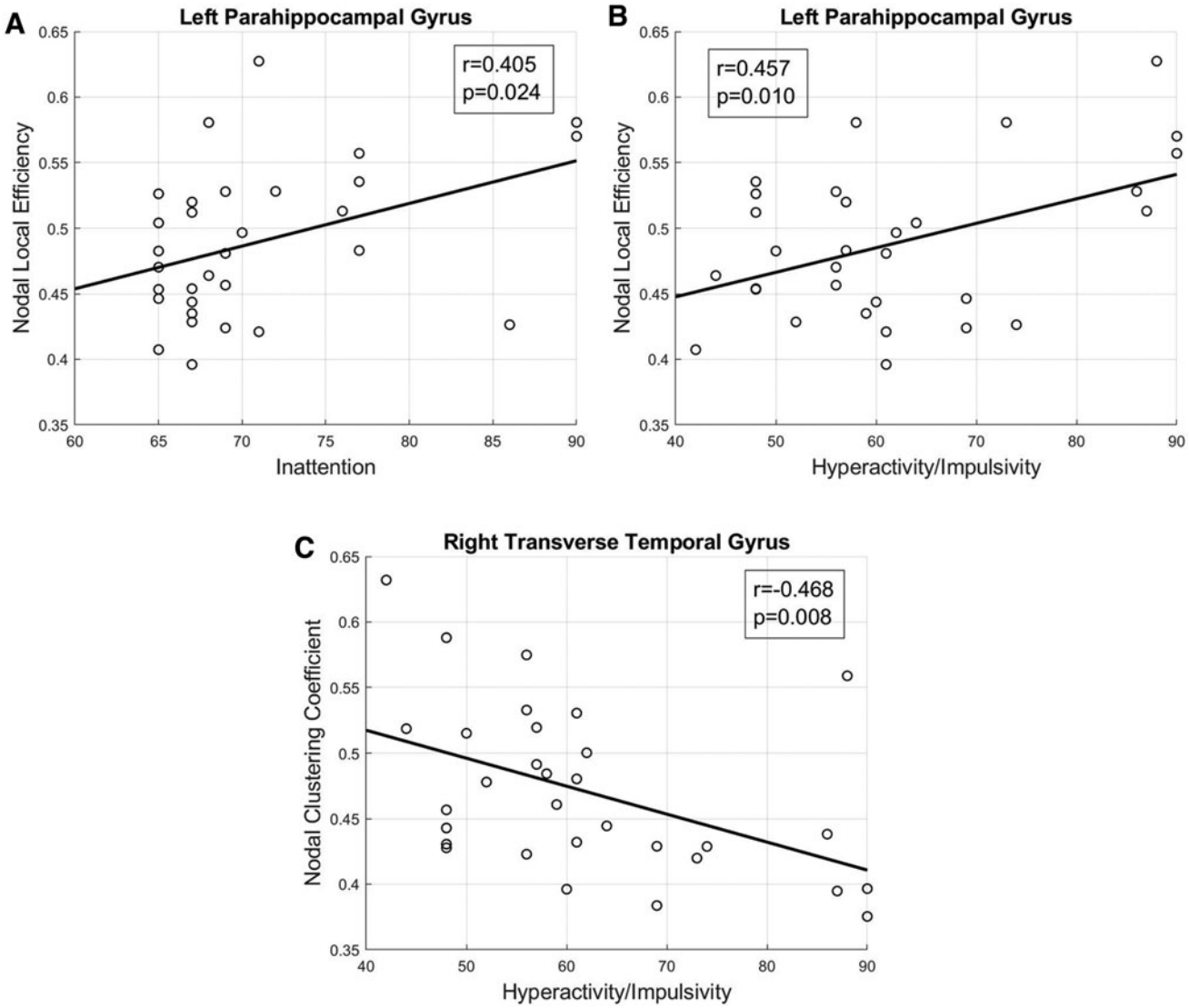

FIG. 3. Regions that showed significant brain-behavior correlations in the TBI-A group. The *p*-values reported in the figure were after Bonferroni correction. **(A)** Correlation between hyperactive/impulsive symptoms severity score and nodal local efficiency of left parahippocampal gyrus. **(B)** Correlation between inattentive symptoms severity score and nodal local efficiency of left parahippocampal gyrus. **(C)** Correlation between hyperactive/impulsive symptoms severity score and nodal lustering coefficient of right transverse temporal gyrus.

chronic TBI children, relative to matched controls (Merkley et al., 2008), whereas a more recent longitudinal study reported significant correlation between greater volume of left supramarginal gyrus and worse overall cognitive performance (Dennis et al., 2016). Meanwhile, task-based functional MRI studies have demonstrated abnormal supramarginal gyrus activation in children with chronic TBI, when performing a motor task (Caeyenberghs et al., 2009) and a working memory task (Newsome et al., 2008). However, similar to the fact from investigations in frontal regions, no evidence has yet suggested strong linkage between parietal lobe GM/WM tissue alterations and post-TBI attention deficits in children.

Intriguingly, this study found that relative to controls, the TBI-A group had significantly decreased nodal local efficiency in left parahippocampal gyrus and significantly increased nodal local efficiency and nodal clustering coefficient in right transverse temporal gyrus. Furthermore, nodal local efficiency in left parahippocampal gyrus showed significant positive correlations with the post-TBI inattentive and hyperactive symptoms, and nodal local efficiency in right transverse temporal gyrus showed significant negative correlations with the post-TBI hyperactive symptoms, in the group of TBI-A. These paradoxes may suggest compensatory or scaffolding mechanisms where reduced efficiency in left parahippocampal gyrus and increased efficiency in right transverse temporal gyrus both illustrate potential structural brain recovery from TBI-induced behavioral impairment in attention domain. Similar to the frontal lobe, temporal lobe is also among the most vulnerable brain regions for DAI, owing to its anatomical location as the close proximity to the bony structure of the middle fossa of the skull (Bigler, 2007). TBI-related cortical GM atrophy and disrupted

WM integrity in temporal lobe have been reported in several studies in children with chronic TBI (Caeyenberghs et al., 2012; Dennis et al., 2016; Diez et al., 2017; Wilde et al., 2005, 2012a). The transverse temporal gyrus, also called Heschl's gyrus, is the primary auditory cortex responsible for early processing related to speech understanding (Arnott and Alain, 2011; Recanzone and Cohen, 2010). It was also found to be part of the dorsal pathway in the bottom-up visual attention stream (Katsuki and Constantinidis, 2014), as well as subject to top-down influences of attention (Voisin et al., 2006). Parahippocampal gyrus belongs to the medial temporal system for visuospatial processing, which has intensive WM connections with frontal, parietal, occipital cortices, and midbrain structures. It was found to involve in selective attention during shifting and orienting processes through the ventral attention pathways (Corbetta and Shulman, 2002; Ochsner et al., 2012; Vossel et al., 2014; Wager et al., 2004). Both the transverse temporal and parahippocampal gyri are critical components in the multisensory integration system for attention processing (Cappe et al., 2009). These existing studies in cognitive neuroscience have provided strong scientific premise of our novel findings in the temporal lobe in children with TBI-A. Therefore, we suggest that TBI-related local re-modularity associated with the transverse temporal region, and structural segregation of the subnetworks connecting the parahippocampal gyrus with other brain regions, may have significant linkage with the onset of post-TBI inattentive and hyperactive/impulsive symptoms in children.

There are some limitations in this study. First, the sample size is relatively modest. Compared with other existing studies with similar sample sizes, the effect size of our study is larger, because of the inclusion criteria of the two diagnostic groups (the T-scores of inattentive and hyperactive subscales were ≥65 for TBI-A, whereas ≤60 for controls). The increased effect size can help improve statistical power of our study. Second, the study did not include a clinical control group of TBI children without clinically significant attention deficits. Therefore, this study by itself could not testify whether the structural anomalies in the TBI-A group might also be seen in TBI patients more generally who do not have attention deficits. Nevertheless, the main findings of this study reviewed in the above paragraphs, the structural alterations in left frontal, supramarginal, and parahippocampal gyri, have also been reported by other research groups to exist in TBI children without showing significant attention deficits (or studies without including post-TBI attention problems as inclusion/exclusion criteria). In addition, previous clinical studies have consistently reported that in children with TBI, 15% develop attention deficits 6–12 months after the injury and 21% during the second year (Max et al., 2005), and >50% from 1 year up to 10 years postinjury (Narad et al., 2018). However, we acknowledge that ADHD is a neurodevelopmental problem that can develop in this age range independently from any TBI episode. Therefore, it cannot be unexclusively concluded that the attention problems reported in these TBI-A children were all TBI induced. To minimize the number of potential primary ADHD subjects, we included detailed parent report to assess the preinjury behavioral problems and have excluded subjects with uncertain responses and subjects with family history of ADHD. Considering the majority of ADHD onset is before age of 7 (Polanczyk et al., 2010), the number of potential primary ADHD in the TBI-A group is minimal. Third, sex-related topological differences of the structural brain network, and their interactions with the two diagnostic groups were not investigated, considering the sample size limitation of the study. Recently, several studies have reported effects of sex and SES on the long-term cognitive and behavioral outcomes in children with TBI (Anderson et al., 2013; Scholten et al., 2015; Wade et al., 2016; Yeates et al., 2012). Additional analyses of our sample did not show any trends of significant correlations of the SES and time from injury with any clinical/behavioral measures in the TBI-A group. To partially remove the potential effects of these factors, we added sex as a fixed-effect covariate, and SES as a random-effect covariate, in the group-level analyses. Future work in a sample with a much larger size and a broader behavioral spectrum in terms of inattentiveness is expected to further elucidate how the results of this study would provide new leads in structural brain network changes associated with post-TBI attention deficits, and their interactions with the critical biological and social environmental factors. Finally, the DTI acquisition parameters were not optimal. The voxel size of our data was $2 \times 2 \times 2.5\ mm^3$. A previous study suggested that anisotropy in the z-plane may affect the estimation of FA values and fiber directions (Oouchi et al., 2007; Soares et al., 2013). In addition, the percentage of voxels that contain at least two crossing fibers was relatively low in this study when compared with a previous one (22% vs. 63%) (Jeurissen et al., 2013). The reduced sensitivity in detecting the orientations of small fibers may be owing to the relative low diffusion weighting (Jones et al., 2013). Because the major long-distance WM tracts are most vulnerable to TBI (Sharp et al., 2014) and both groups were applied with same settings, this limitation should not bias the group comparison.

In summary, this study demonstrated significantly altered regional topological organizations of the WM brain network in frontal, parietal, and temporal regions, in a more homogeneous subgroup of children with chronic TBI who had severe post-TBI attention deficits. The results further suggest that TBI-related WM structural re-modularity in the subnetworks associated with temporal lobe may significantly link to onset of severe post-TBI attention deficits in the affected children. These findings provide valuable implication for understanding the neurobiological substrates of post-TBI attention deficits, and have the potential to serve as quantitatively measurable criteria guiding the development of more timely and tailored strategies for diagnoses and treatments to the affected individuals.

Authors' Contributions

X.L. designed the study. M.C. worked on literature searching, clinical and imaging data analyses, and wrote the first draft of the article. Y.L. and Z.W. contributed to data acquisition. X.L., J.M.H., C.A.M., L.C., Y.L., Z.W., B.B., and T.L.A. edited and revised the article. All authors contributed to and have approved the final version of the article.

Author Disclosure Statement

No competing financial interests exist.

Funding Information

This work was partially supported by research grants from the National Institute of Mental Health (R03MH109791,

R15MH117368), the New Jersey Commission on Brain Injury Research (CBIR17PIL012), and the New Jersey Institute of Technology Start-up Award.

References

Adamson C, Yuan W, Babcock L, et al. 2013. Diffusion tensor imaging detects white matter abnormalities and associated cognitive deficits in chronic adolescent TBI. Brain Inj 27: 454–463.

American Psychiatric Association. 2013. *Diagnostic and statistical manual of mental disorders: DSM-5*. Arlington, VA: American Psychiatric Publishing.

Anderson V, Beauchamp MH, Yeates KO, et al. 2013. Social competence at 6 months following childhood traumatic brain injury. J Int Neuropsychol Soc 19:539–550.

Andersson JLR, Sotiropoulos SN. 2016. An integrated approach to correction for off-resonance effects and subject movement in diffusion MR imaging. Neuroimage 125:1063–1078.

Arnott SR, Alain C. 2011. The auditory dorsal pathway: orienting vision. Neurosci Biobehav Rev 35:2162–2173.

Backeljauw B, Kurowski BG. 2014. Interventions for attention problems after pediatric traumatic brain injury: what is the evidence? PM R 6:814–824.

Bassett DS, Wymbs NF, Porter MA, et al. 2011. Dynamic reconfiguration of human brain networks during learning. Proc Natl Acad Sci U S A 108:7641–7646.

Bathelt J, Johnson A, Zhang M, et al. 2019. The cingulum as a marker of individual differences in neurocognitive development. Sci Rep 9:2281.

Baum GL, Ciric R, Roalf DR, et al. 2017. Modular segregation of structural brain networks supports the development of executive function in youth. Curr Biol 27:1561–1572 e1568.

Behrens TE, Berg HJ, Jbabdi S, et al. 2007. Probabilistic diffusion tractography with multiple fibre orientations: what can we gain? Neuroimage 34:144–155.

Bigler ED. 2007. Anterior and middle cranial fossa in traumatic brain injury: relevant neuroanatomy and neuropathology in the study of neuropsychological outcome. Neuropsychology 21:515–531.

Bigler ED, Abildskov TJ, Petrie J, et al. 2013. Heterogeneity of brain lesions in pediatric traumatic brain injury. Neuropsychology 27:438–451.

Blakemore SJ, Choudhury S. 2006. Development of the adolescent brain: implications for executive function and social cognition. J Child Psychol Psychiatry 47:296–312.

Caeyenberghs K, Leemans A, De Decker C, et al. 2012. Brain connectivity and postural control in young traumatic brain injury patients: a diffusion MRI based network analysis. Neuroimage Clin 1:106–115.

Caeyenberghs K, Leemans A, Leunissen I, et al. 2013. Topological correlations of structural and functional networks in patients with traumatic brain injury. Front Hum Neurosci 7:726.

Caeyenberghs K, Leemans A, Leunissen I, et al. 2014. Altered structural networks and executive deficits in traumatic brain injury patients. Brain Struct Funct 219:193–209.

Caeyenberghs K, Wenderoth N, Smits-Engelsman BC, et al. 2009. Neural correlates of motor dysfunction in children with traumatic brain injury: exploration of compensatory recruitment patterns. Brain 132:684–694.

Cappe C, Rouiller EM, Barone P. 2009. Multisensory anatomical pathways. Hear Res 258:28–36.

Carskadon MA, Acebo C. 1993. A self-administered rating scale for pubertal development. J Adolesc Health 14:190–195.

Chu SH, Parhi KK, Lenglet C. 2018. Function-specific and enhanced brain structural connectivity mapping via joint modeling of diffusion and functional MRI. Sci Rep 8:4741.

Conners CK. 2008. *Conners*, 3rd ed. North Tonawanda, NY: Multi-Health Systems.

Corbetta M, Shulman GL. 2002. Control of goal-directed and stimulus-driven attention in the brain. Nat Rev Neurosci 3: 201–215.

Dall'acqua P, Johannes S, Mica L, et al. 2017. Functional and structural network recovery after mild traumatic brain injury: a 1-Year longitudinal study. Front Hum Neurosci 11:280.

Dennis EL, Hua X, Villalon-Reina J, et al. 2016. Tensor-based morphometry reveals volumetric deficits in moderate = severe pediatric traumatic brain injury. J Neurotrauma 33:840–852.

Dennis EL, Jin Y, Villalon-Reina JE, et al. 2015. White matter disruption in moderate/severe pediatric traumatic brain injury: advanced tract-based analyses. Neuroimage Clin 7:493–505.

De Reus MA, Van Den Heuvel MP. 2013. Estimating false positives and negatives in brain networks. Neuroimage 70:402–409.

Dewan MC, Mummareddy N, Wellons JC, III, et al. 2016. Epidemiology of global pediatric traumatic brain injury: qualitative review. World Neurosurg 91:497–509 e491.

Diez I, Drijkoningen D, Stramaglia S, et al. 2017. Enhanced prefrontal functional-structural networks to support postural control deficits after traumatic brain injury in a pediatric population. Netw Neurosci 1:116–142.

Eckner JT, Kutcher JS, Richardson JK. 2011. Effect of concussion on clinically measured reaction time in 9 NCAA division I collegiate athletes: a preliminary study. PM R 3:212–218.

Ewing-Cobbs L, Johnson CP, Juranek J, et al. 2016. Longitudinal diffusion tensor imaging after pediatric traumatic brain injury: impact of age at injury and time since injury on pathway integrity. Hum Brain Mapp 37:3929–3945.

Ewing-Cobbs L, Prasad MR, Swank P, et al. 2008. Arrested development and disrupted callosal microstructure following pediatric traumatic brain injury: relation to neurobehavioral outcomes. Neuroimage 42:1305–1315.

Faber J, Wilde EA, Hanten G, et al. 2016. Ten-year outcome of early childhood traumatic brain injury: diffusion tensor imaging of the ventral striatum in relation to executive functioning. Brain Inj 30:1635–1641.

Fagerholm ED, Hellyer PJ, Scott G, et al. 2015. Disconnection of network hubs and cognitive impairment after traumatic brain injury. Brain 138:1696–1709.

Fischl B. 2012. FreeSurfer. Neuroimage 62:774–781.

Freeman LCJSN. 1978. Centrality in social networks conceptual clarification. 1:215–239.

Green GH, Diggle PJ. 2007. On the operational characteristics of the Benjamini and Hochberg false discovery rate procedure. Stat Appl Genet Mol Biol 6:Article27.

Hellyer PJ, Scott G, Shanahan M, et al. 2015. Cognitive flexibility through metastable neural dynamics is disrupted by damage to the structural connectome. J Neurosci 35:9050–9063.

Imms P, Clemente A, Cook M, et al. 2019. The structural connectome in traumatic brain injury: a meta-analysis of graph metrics. Neurosci Biobehav Rev 99:128–137.

Jenkinson M, Beckmann CF, Behrens TE, et al. 2012. Fsl. Neuroimage 62:782–790.

Jeurissen B, Leemans A, Tournier JD, et al. 2013. Investigating the prevalence of complex fiber configurations in white

matter tissue with diffusion magnetic resonance imaging. Hum Brain Mapp 34:2747–2766.
Jolly AE, Scott GT, Sharp DJ, et al. 2020. Distinct patterns of structural damage underlie working memory and reasoning deficits after traumatic brain injury. Brain 143:1158–1176.
Jones DK, Knosche TR, Turner R. 2013. White matter integrity, fiber count, and other fallacies: the do's and don'ts of diffusion MRI. Neuroimage 73:239–254.
Katsuki F, Constantinidis C. 2014. Bottom-up and top-down attention: different processes and overlapping neural systems. Neuroscientist 20:509–521.
Kaufman J, Birmaher B, Brent DA, et al. 2000. K-Sads-Pl. J Am Acad Child Adolesc Psychiatry 39:1208.
Kim J, Parker D, Whyte J, et al. 2014. Disrupted structural connectome is associated with both psychometric and real-world neuropsychological impairment in diffuse traumatic brain injury. J Int Neuropsychol Soc 20:887–896.
Konigs M, Heij HA, Van Der Sluijs JA, et al. 2015. Pediatric traumatic brain injury and attention deficit. Pediatrics 136: 534–541.
Konigs M, Pouwels PJ, Ernest Van Heurn LW, et al. 2018. Relevance of neuroimaging for neurocognitive and behavioral outcome after pediatric traumatic brain injury. Brain Imaging Behav 12:29–43.
Konigs M, Van Heurn LWE, Bakx R, et al. 2017. The structural connectome of children with traumatic brain injury. Hum Brain Mapp 38:3603–3614.
Kramer ME, Chiu CY, Walz NC, et al. 2008. Long-term neural processing of attention following early childhood traumatic brain injury: fMRI and neurobehavioral outcomes. J Int Neuropsychol Soc 14:424–435.
Kuceyeski AF, Jamison KW, Owen JP, et al. 2019. Longitudinal increases in structural connectome segregation and functional connectome integration are associated with better recovery after mild TBI. Hum Brain Mapp 40:4441–4456.
Kurowski B, Wade SL, Cecil KM, et al. 2009. Correlation of diffusion tensor imaging with executive function measures after early childhood traumatic brain injury. J Pediatr Rehabil Med 2:273–283.
Kurowski BG, Epstein JN, Pruitt DW, et al. 2019. Benefits of methylphenidate for long-term attention problems after traumatic brain injury in childhood: a randomized, double-masked, placebo-controlled, dose-titration, crossover trial. J Head Trauma Rehabil 34:E1–E12.
Latora V, Marchiori M. 2001. Efficient behavior of small-world networks. Phys Rev Lett 87:198701.
Leblond E, Smith-Paine J, Riemersma JJ, et al. 2019. Influence of methylphenidate on long-term neuropsychological and everyday executive functioning after traumatic brain injury in children with secondary attention problems. J Int Neuropsychol Soc 25:740–749.
Le Fur C, Camara-Costa H, Francillette L, et al. 2020. Executive functions and attention 7 years after severe childhood traumatic brain injury: results of the Traumatisme Grave de l'Enfant (TGE) cohort. Ann Phys Rehabil Med 63:270–279.
Lindsey HM, Lalani SJ, Mietchen J, et al. 2019. Acute pediatric traumatic brain injury severity predicts long-term verbal memory performance through suppression by white matter integrity on diffusion tensor imaging. Brain Imaging Behav 2020;14:1626–1637.
Lipszyc J, Levin H, Hanten G, et al. 2014. Frontal white matter damage impairs response inhibition in children following traumatic brain injury. Arch Clin Neuropsychol 29:289–299.
Lumba-Brown A, Yeates KO, Sarmiento K, et al. 2018. Diagnosis and management of mild traumatic brain injury in children: a systematic review. JAMA Pediatr 172:e182847.
Max JE, Schachar RJ, Levin HS, et al. 2005. Predictors of secondary attention-deficit/hyperactivity disorder in children and adolescents 6 to 24 months after traumatic brain injury. J Am Acad Child Adolesc Psychiatry 44:1041–1049.
Mayer AR, Hanlon FM, Ling JM. 2015. Gray matter abnormalities in pediatric mild traumatic brain injury. J Neurotrauma 32:723–730.
Merkley TL, Bigler ED, Wilde EA, et al. 2008. Diffuse changes in cortical thickness in pediatric moderate-to-severe traumatic brain injury. J Neurotrauma 25:1343–1345.
Mishra VR, Sreenivasan KR, Zhuang X, et al. 2019. Understanding white matter structural connectivity differences between cognitively impaired and nonimpaired active professional fighters. Hum Brain Mapp 40:5108–5122.
Misic B, Betzel RF, Griffa A, et al. 2018. Network-based asymmetry of the Human Auditory System. Cereb Cortex 28:2655–2664.
Mitra J, Shen KK, Ghose S, et al. 2016. Statistical machine learning to identify traumatic brain injury (TBI) from structural disconnections of white matter networks. Neuroimage 129:247–259.
Molteni E, Pagani E, Strazzer S, et al. 2019. Fronto-temporal vulnerability to disconnection in paediatric moderate and severe traumatic brain injury. Eur J Neurol 26:1183–1190.
Narad ME, Kennelly M, Zhang N, et al. 2018. Secondary attention-deficit/hyperactivity disorder in children and adolescents 5 to 10 years after traumatic brain injury. JAMA Pediatr 172:437–443.
Narad ME, Riemersma J, Wade SL, et al. 2019. Impact of secondary ADHD on long-term outcomes after early childhood traumatic brain injury. J Head Trauma Rehabil 2020;35: E271–E279.
Newsome MR, Steinberg JL, Scheibel RS, et al. 2008. Effects of traumatic brain injury on working memory-related brain activation in adolescents. Neuropsychology 22:419–425.
Ochsner KN, Silvers JA, Buhle JT. 2012. Functional imaging studies of emotion regulation: a synthetic review and evolving model of the cognitive control of emotion. Ann N Y Acad Sci 1251:E1–E24.
Oldfield RC. 1971. The assessment and analysis of handedness: the Edinburgh inventory. Neuropsychologia 9:97–113.
Onnela JP, Saramaki J, Kertesz J, et al. 2005. Intensity and coherence of motifs in weighted complex networks. Phys Rev E Stat Nonlin Soft Matter Phys 71:065103.
Oouchi H, Yamada K, Sakai K, et al. 2007. Diffusion anisotropy measurement of brain white matter is affected by voxel size: underestimation occurs in areas with crossing fibers. AJNR Am J Neuroradiol 28:1102–1106.
Polanczyk G, Caspi A, Houts R, et al. 2010. Implications of extending the ADHD age-of-onset criterion to age 12: results from a Prospectively Studied Birth Cohort. J Am Acad Child Adolesc Psychiatry 49:210–216.
Polinder S, Haagsma JA, Van Klaveren D, et al. 2015. Health-related quality of life after TBI: a systematic review of study design, instruments, measurement properties, and outcome. Popul Health Metr 13:4.
Raizman R, Tavor I, Biegon A, et al. 2020. Traumatic brain injury severity in a network perspective: a diffusion MRI based Connectome Study. Sci Rep 10:9121.
Recanzone GH, Cohen YE. 2010. Serial and parallel processing in the primate auditory cortex revisited. Behav Brain Res 206:1–7.

Roberts RM, Mathias JL, Rose SE. 2016. Relationship between diffusion tensor imaging (DTI) findings and cognition following pediatric TBI: a meta-analytic review. Dev Neuropsychol 41:176–200.

Rubinov M, Sporns O. 2010. Complex network measures of brain connectivity: uses and interpretations. Neuroimage 52:1059–1069.

Rubinov M, Sporns O. 2011. Weight-conserving characterization of complex functional brain networks. Neuroimage 56: 2068–2079.

Scholten AC, Haagsma JA, Andriessen TM, et al. 2015. Health-related quality of life after mild, moderate and severe traumatic brain injury: patterns and predictors of suboptimal functioning during the first year after injury. Injury 46:616–624.

Sharp DJ, Scott G, Leech R. 2014. Network dysfunction after traumatic brain injury. Nat Rev Neurol 10:156–166.

Soares JM, Marques P, Alves V, et al. 2013. A hitchhiker's guide to diffusion tensor imaging. Front Neurosci 7:31.

Spreng RN, Sepulcre J, Turner GR, et al. 2013. Intrinsic architecture underlying the relations among the default, dorsal attention, and frontoparietal control networks of the human brain. J Cogn Neurosci 25:74–86.

Strazzer S, Rocca MA, Molteni E, et al. 2015. Altered recruitment of the attention network is associated with disability and cognitive impairment in pediatric patients with acquired brain injury. Neural Plast 2015:104282.

Teasdale G, Jennett B. 1974. Assessment of coma and impaired consciousness. A practical scale. Lancet 2:81–84.

Tlustos SJ, Chiu CY, Walz NC, et al. 2011. Neural correlates of interference control in adolescents with traumatic brain injury: functional magnetic resonance imaging study of the counting stroop task. J Int Neuropsychol Soc 17:181–189.

Treble A, Hasan KM, Iftikhar A, et al. 2013. Working memory and corpus callosum microstructural integrity after pediatric traumatic brain injury: a diffusion tensor tractography study. J Neurotrauma 30:1609–1619.

Verhelst H, Vander Linden C, De Pauw T, et al. 2018. Impaired rich club and increased local connectivity in children with traumatic brain injury: local support for the rich? Hum Brain Mapp 39:2800–2811.

Voisin J, Bidet-Caulet A, Bertrand O, et al. 2006. Listening in silence activates auditory areas: a functional magnetic resonance imaging study. J Neurosci 26:273–278.

Vossel S, Geng JJ, Fink GR. 2014. Dorsal and ventral attention systems: distinct neural circuits but collaborative roles. Neuroscientist 20:150–159.

Wade SL, Zhang N, Yeates KO, et al. 2016. Social Environmental moderators of long-term functional outcomes of early childhood brain injury. JAMA Pediatr 170:343–349.

Wager TD, Jonides J, Reading S. 2004. Neuroimaging studies of shifting attention: a meta-analysis. Neuroimage 22:1679–1693.

Watson CG, Demaster D, Ewing-Cobbs L. 2019. Graph theory analysis of DTI tractography in children with traumatic injury. Neuroimage Clin 21:101673.

Wechsler D. 2011. *Wechsler Abbreviated Scale of Intelligence–Second Edition (WASI-II)*. San Antonio, TX: NCS Pearson.

Wilde EA, Ayoub KW, Bigler ED, et al. 2012a. Diffusion tensor imaging in moderate-to-severe pediatric traumatic brain injury: changes within an 18 month post-injury interval. Brain Imaging Behav 6:404–416.

Wilde EA, Hunter JV, Newsome MR, et al. 2005. Frontal and temporal morphometric findings on MRI in children after moderate to severe traumatic brain injury. J Neurotrauma 22:333–344.

Wilde EA, Merkley TL, Bigler ED, et al. 2012b. Longitudinal changes in cortical thickness in children after traumatic brain injury and their relation to behavioral regulation and emotional control. Int J Dev Neurosci 30:267–276.

Wilde EA, Newsome MR, Bigler ED, et al. 2011. Brain imaging correlates of verbal working memory in children following traumatic brain injury. Int J Psychophysiol 82: 86–96.

Wozniak JR, Krach L, Ward E, et al. 2007. Neurocognitive and neuroimaging correlates of pediatric traumatic brain injury: a diffusion tensor imaging (DTI) study. Arch Clin Neuropsychol 22:555–568.

Yeates KO, Taylor HG, Rusin J, et al. 2012. Premorbid child and family functioning as predictors of post-concussive symptoms in children with mild traumatic brain injuries. Int J Dev Neurosci 30:231–237.

Yuan W, Treble-Barna A, Sohlberg MM, et al. 2017a. Changes in structural connectivity following a cognitive intervention in children with traumatic brain injury. Neurorehabil Neural Repair 31:190–201.

Yuan W, Wade SL, Babcock L. 2015. Structural connectivity abnormality in children with acute mild traumatic brain injury using graph theoretical analysis. Hum Brain Mapp 36: 779–792.

Yuan W, Wade SL, Quatman-Yates C, et al. 2017b. Structural connectivity related to persistent symptoms after mild TBI in adolescents and response to aerobic training: preliminary investigation. J Head Trauma Rehabil 32:378–384.

Address correspondence to:
Xiaobo Li
Department of Biomedical Engineering
New Jersey Institute of Technology
323 Martin Luther King Blvd., Fenster 613
Newark, NJ 07102
USA

E-mails: xli.aecom@gmail.com; xiaobo.li@njit.edu